# ANALYTICAL MODEL FOR PREDICTING PRESTRESS TRANSFER BOND-RELATED PARAMETERS OF 18 MM PRESTRESSING STRANDS

Ahmed Almohammedi[1], Rahman S. Kareem[1,2], Canh N. Dang[3],
José R. Martí-Vargas[4*], and W. Micah Hale[1]

[1] Department of Civil Engineering, University of Arkansas, Fayetteville, AR 72701, USA
[2] Department of Structure, Shatrah Technical Institute, Southern Technical University, Shatrah, Dhi Qar, Iraq
[3] Thornton Tomasetti, Ho Chi Minh City, Vietnam
[3] Institute of Concrete Science and Technology (ICITECH), Universitat Politècnica de València, 4G, Camino de Vera s/n, 46022 Valencia, Spain

* Corresponding author: Email: jrmarti@cst.upv.es

## ABSTRACT

The bond between prestressing strand and concrete is necessary for the composite-action of the two materials. This study develops an analytical model to investigate the bond performance of 18-mm prestressing strands. The model considers the concrete compressive strength for both conventional and self-consolidating concrete. It is then used to determine the short- (at prestress transfer) and the long-term (after all prestress losses) transfer length and strand end slip. The predicted short-term transfer length and strand slip values were validated with the experimental results obtained from several pretensioned concrete beams and girders, which had various geometric configurations, concrete compressive strength, and number of prestressing strands. The results showed that the model provided a reasonable prediction of bond performance. From the analysis of the predicted long-term transfer length and strand end slip values, the long-term transfer length is on average 33% longer than the short-term transfer length, whereas the increase in strand end slip is on average 24% from the short- to the long-term stage. Regardless of concrete compressive strength and concrete type (conventional and self-consolidating concrete), both the ACI-318 and AASHTO LFRD codes provided a conservative limit for the predicted long-term transfer length values.

**KEYWORDS**

pretensioned concrete; bond model; prestressing strand; 18-mm strand; transfer length; slip

## 1. INTRODUCTION

When compared to reinforced concrete, pretensioned concrete is one of the dominant materials in long-span structures. The use of high or ultra-high strength prestressing strand is the driving factor. The yield strength of those strands (Grade 1860, 2200, and 24000) is assumed to be 90% of its ultimate strength ($f_{pu}$) [1–3], and is about 4 or 5 times greater than that of Grade 420 reinforcing bar. To fully utilize the high-strength capacity, the prestressing strand is pretensioned before casting concrete. Once the concrete reaches the compressive strength required for prestress transfer, the prestressing strand is released. The bond at the interface of the prestressing strand and concrete is crucial for transferring the prestress force from the strand to the surrounding concrete material. In terms of structural design, the strand bond has a direct correlation to transfer length (or transmission length); a significant design parameter at the prestress transfer state and ultimate limit state [4,5]. Strand bond is comprised of three factors: adhesion, friction, and mechanical interlocking. Adhesion is a form of chemical bond, formed on the surface of the prestressing strand during the setting of fresh concrete. Friction is a form of bearing stress, also known as the Hoyer's effect [6], which is generated by the lateral expansion of the prestressing strand at prestress transfer. The mechanical interlock is also a form of bearing stress, but generated by the resistance of the hardened concrete to the longitudinal movement of the prestressing strand. The latter two components have a major contribution to the bond strength [7–9]. These bond components are affected by several factors, which typically include concrete compressive strength at prestress transfer, strand surface condition, and strand diameter [10–16]. A direct measurement of strand bond, for example by attaching strain gauges to the prestressing strand surface, may be not feasible as the gauges can distort the bond phenomenon and also become damaged during concrete casting. An indirect method is to develop a strand bond model, which typically consists of a set of mathematical equations to represent the interaction between the prestressing strand and concrete. The bond model can be used to implement finite-element modeling [17–22]. An analytical investigation is an alternative technique which provides similar outcomes [23–29]. Typical results consist of transfer length, strand slip, bond stress distribution, and strand stress variation of the prestressing strand. In fact, transfer length and strand slip are the parameters of interest, since they can be experimentally measured by reliable techniques for validating the analytical model [7,30–32].

Within the transfer zone, the prestress force in the prestressing strand is assumed to be linearly transferred to the surrounding concrete. When the transfer stage ends, the length of the transfer zone is technically termed as the transfer length, which is depicted in Figure 1. The significance of transfer length in the design of pretensioned concrete members is demonstrated through two aspects: (a) a short transfer length implies high compressive stresses and a risk of cracking at the member ends; and (b) a long transfer length negatively affects the shear strength and flexural capacity of the members. The ACI 318 [33] indicates that transfer length can be calculated using Eq. (1), which considers the effective stress ($f_{se}$) and strand diameter ($d_b$) as the two key parameters in the prediction. This equation was developed based on an assumption of constant bond stress of 2.76 MPa (400 psi) [34]. Alternatively, transfer length can be simply estimated as 50$d_b$. In a similar way, the AASHTO LRFD Bridge Design Specifications [35] also proposes the transfer length as 60$d_b$.

$$L_t = \frac{1}{20.7} f_{se} d_b \quad (f_{se} \text{ in MPa}) \qquad (1)$$

$$L_t = \frac{1}{3} f_{se} d_b \quad (f_{se} \text{ in ksi})$$

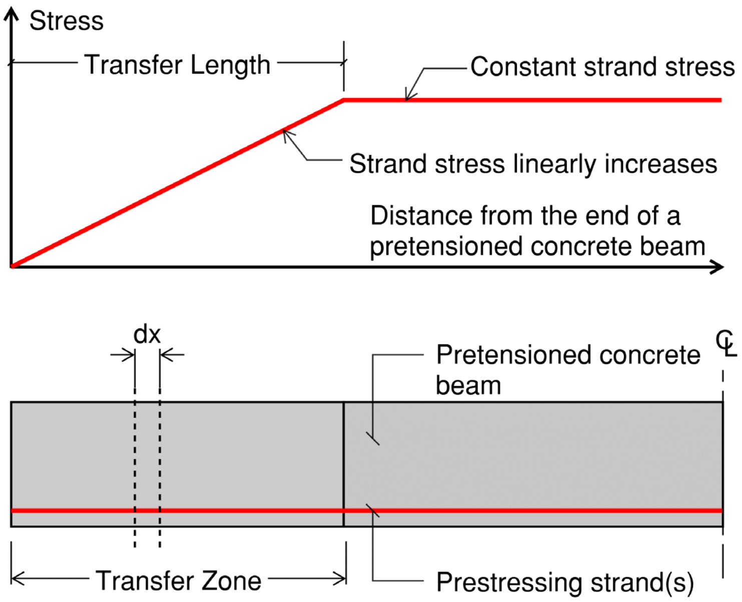


Figure 1 - Transfer length and strand stress variation

Typical 7-wire prestressing steel strands, 13-mm and 15-mm nominal diameter, have been used for pretensioned concrete applications for years. The use of 18-mm prestressing strand has been only investigated recently. The prestress force provided by a 18-mm prestressing strand is 38% and 93% greater than that provided by a 15-mm and 13-mm strand, respectively. The use of the larger strands (18 mm) offers several advantages, such as reducing the number of required strands and reducing girder depth and weight. The structural efficiency of using 18-mm strands in bridge design and construction has been demonstrated in a few projects in the U.S. [36,37]. However, the lack of the strand performance data and the lack of design specifications have limited their use in the precast, prestressed concrete industry. In fact, recent studies recommend further research to increase the database of experimental results regarding the bond phenomena in self-consolidating concrete [15,16].

The research presented in this paper develops a strand bond model to predict transfer length and end slip for beams containing 18-mm prestressing strands cast in conventional or self-consolidating concrete. The experimental data from two testing methodologies have been used to validate and calibrate the proposed model: pullout forces from the North American Strand Producers (NASP) Bond Test ─adopted by American Society for Testing Materials (ASTM) as Standard Test for Strand Bond (STSB) [38]─ and the transfer length and strand slip measured in pretensioned concrete beams and girders.

## 2. LITERATURE REVIEW

Strand bond models have been developed throughout last two decades through extensive research efforts. Balazs's research [39] is one of the first studies focusing on developing a bond model for prestressing strand. The bond stress was considered to be a function of strand slip. Through solving a set of nonlinear equations, a closed-form solution of transfer length was achieved. However, two shortcomings exist: (a) the bond model was not based on any previous experimental investigation; and (b) no experimental data were presented for verification of the proposed transfer length equation. Den Uijl [40] refined the strand bond model by using the results of pull-out and push-in tests. The bond stress is a function of strand slip and variation of strand stress and strain. The model was then used to develop a transfer length equation. The lack of experimental verification for the predicted transfer length is a limitation of the study.

Park and Cho [41] developed a strand bond model and experimentally verified the model's applicability. The experimental study involved casting several 3-m long pretensioned concrete prisms with a cross section of either 120×120 mm or 150×150 mm. Each prism contained one 13-mm or 15-mm prestressing strand. The predicted transfer length was in a good agreement with the test results for the investigated prestressing strands. Martí-Vargas *et al.* [42] further investigated the strand slip along the transmission and anchorage lengths of pretensioned concrete members using an analytical model. This model was derived from experimental research work, which involved measuring the strand end slip, the prestress force, and transmission and the anchorage lengths. A single 13-mm prestressing strand was embedded in the test specimens that had a cross-section of 100×100 mm. The model was assessed using theoretical equations and experimental results from the literature. The study proposed an analytical bond model to predict the slip distribution of 13-mm prestressing strands within the transfer length. In fact, these two studies have a similar shortcoming, in which the experimental verification was conducted on small-scale pretensioned concrete members or small-size prestressing strands.

Dang *et al.* [43] developed a model for 15-mm prestressing strand by using the test results of the Standard Test for Strand Bond (STSB) specified by ASTM A1081 [38]. The STSB is able to provide a reliable indication of the bond condition of prestressing strand [9]. The effect of concrete compressive strength was additionally considered in the strand bond model. These are two dominant factors affecting strand bond. As a result, the model provided a reasonable transfer-length prediction from an experimental database of 19 pretensioned concrete beams. These data were collected from similar studies of 45 beams cast at the University of Arkansas. The researchers found that the transfer length predicted by ACI 318 limit of $50d_b$ is conservative if the concrete has compressive strength of 26.7 MPa (4 ksi) or greater at prestress transfer. Despite these findings, one main limitation is that the conclusion is only applicable for the transfer length at prestress transfer. To overcome the limitation, Kareem *et al.* [44] further refined the proposed model by considering the effect of concrete creep and shrinkage to the long-term performance of strand bond. It was analytically determined that the transfer length of the prestressing strand can increase by 20% during the first 28 days of age, which is consistent with experimental study conducted by Barnes *et al.* [11]. On the other hand, it was observed that the transfer length can increase by 25% after one year of age and then remain nearly constant. Regardless of the specific findings for 15-mm prestressing strand, Kareem *et al.* [44] posts a concern about the effect of concrete creep and shrinkage to the long-term strand bond performance.

Regarding the bond performance of 18-mm prestressing strand, an important issue is that the diameter is 17% and 40% greater than 15-mm and 13-mm strands, respectively. As observed in Eq. (1), the strand diameter is considered a main parameter, which determines the strand perimeter in contact with the surrounding concrete. It should be noted that a greater strand diameter (and perimeter) improves bond performance linearly. However, if the prestress level introduced in the strands is the same, which typically corresponds to $0.75f_{pu}$ as a maximum established in manuals and design codes, a greater strand diameter (and area) results in a worse bond condition [34]. As the area/perimeter ratios are 2.56, 2.18, and 1.88 for 18-mm, 15-mm, and 13-mm prestressing strands, respectively, the worst bond condition and then the greater transfer length correspond to 18-mm prestressing strands, which present the higher area/perimeter ratio.

## 3. RESEARCH SIGNIFICANCE

A strand bond model is developed for 18-mm, Grade 1860 prestressing strand. The bond stress function is derived from the STSB data. A calibration factor is adopted to account for the difference in the bond mechanism between the pretensioned prestressing strand used in pretensioned concrete members and the non-pretensioned prestressing strand used in the STSB. The transfer length and strand slip are the parameters of interest derived from the strand bond model. The database for verification included 24 pretensioned concrete beams cast with high-strength conventional concrete or self-consolidating concrete, and a number of medium to large-scale pretension concrete girders cast with a wide range of concrete strengths. The applications and limitations of the developed model are discussed at the end of the research.

## 4. ANALYTICAL APPROACH

Equation (2) is the general form of the strand bond equation [43]. The bond stress *u(x)* at the *x* location in the transfer zone is exponentially proportional to the strand slip *s(x)* through the $\alpha$ coefficient. The bond magnitude of the non-pretensioned prestressing strand is represented by $u_f$. The coefficient $k_b$ represents a calibration coefficient, which is used to calibrate the difference in the bond mechanisms as discussed below.

$$u(x) = k_b u_f \left[ \frac{s(x)}{s_f} \right]^{\alpha} \quad (2)$$

For pretensioned prestressing strand in a concrete member, Hoyer's effect and mechanical interlock simultaneously contribute to the bond magnitude as aforementioned. For the non-pretensioned prestressing strand in the STSB, the mechanical interlock is the only component contributing to the bond magnitude. Pozolo and Andrawes [45] proposed a calibration coefficient $k_b$ of 1.9 for 13-mm prestressing strand. The finite element analysis performed for verification showed a strong correlation to the test results. Dang *et al.* [43] investigated the applicability of the coefficient proposed by Pozolo and Andrawes in the development of a bond model for 15-mm prestressing strand. The predicted transfer length was in agreement with the experimental data. From these findings, it was determined that the calibration coefficient can be independent from the diameter of prestressing strands. In this study, this coefficient is adopted for 18-mm prestressing strand.

### 4.1. Standard Test for Strand Bond

The STSB test procedure is presented in detail in ASTM A1081 [38]. Therefore, only a brief description is provided in this section. A non-pretensioned prestressing strand sample is cast in the center of a steel tube. The tube is 125-mm in diameter and 450-mm in length. A debonded region of 50 mm is provided near the base plate of the steel tube. Accordingly, the embedment length of the strand sample is 400 mm. The steel tube is filled with mortar ─a mixture of sand, cement, and water, which has compressive strength in a range of 31.1 MPa to 34.5 MPa at the time the strand sample is tested. The STSB is performed 24 plus/minus 2 hours after casting by applying a pullout force at one end and measuring strand slip at the other end. The pullout force corresponding to the initial strand end-slip of 0.25 mm ($s_i$) is the initial pullout force ($P_i$). The pullout force corresponding to the final strand end-slip of 2.5 mm ($s_f$) is the final pullout force ($P_f$). The final pullout forces of six samples are averaged and reported as the STSB pullout force.

The exponential coefficient $\alpha$ in Eq. (2) is derived from two data points of STSB as shown in Eq. (3): ($s_i$, $u_i$) and ($s_f$, $u_f$); where $u_i$ and $u_f$ are the bond stresses corresponding to the free-end slips of $s_i$ and $s_f$. respectively. Since the bond stress is proportional to the strand pullout force, Eq. (3) can be re-written as shown in Eq. (4). Based on the investigation of a number of STSB tests, Dang *et al.* [43] determined that the average ratio of $P_i$ to $P_f$ is 0.7. Accordingly, the coefficient $\alpha$ is equal to 0.155. On the other hand, Eq. (2) can be simplified as shown in Eq. (5), where $F_b$ is termed as the bond magnitude given in Eq. (6).

$$\alpha = \frac{\ln\left(u_i/u_f\right)}{\ln\left(s_i/s_f\right)} \tag{3}$$

$$\alpha = \frac{\ln\left(P_i/P_f\right)}{\ln\left(s_i/s_f\right)} \tag{4}$$

$$u(x) = F_b \times s^{\alpha}(x) \tag{5}$$

$$F_b = k_b \frac{u_f}{s_f^{\alpha}} \tag{6}$$

The final pullout force $P_f$, which is used to calculate the final bond stress $u_f$, is based on the research conducted by Morcous and Tadros [46]. A total of 58 pullout tests were performed following similar testing procedures to those of ASTM A1081 [38]. Along with the mortar mixture as specified by the standard, concrete was additionally used for the tests. For the mortar, the cube compressive strength varied from 31 MPa to 34.5 MPa at one-day of age. For the concrete, the 1-day compressive strength ranged from 27.6 MPa to 69.0 MPa. The test results indicated that the STSB pullout force is a function of concrete compressive strength; the higher the concrete strength, the greater the pullout force.

### 4.2. Development of bond model

The stress distribution along an element length *dx* within the transfer zone is described in Figure 2. The specified parameters are defined in the notation list. The force equilibrium equations of the bond stress ($u$) to the concrete stress ($f_c$) and to the strand stress ($f_s$) are presented in Eqs. (7) and (8), respectively. The determination of strand slip, a relative displacement between the strand and the concrete, is shown in Eq. (9). By differentiating Eq. (9) and substituting Eqs. (7) and (8), the relationship of slip and bond stress at position $x$ is obtained as shown in Eq. (10). Eq. (11) is re-written from Eq. (10) by substituting Eq. (4) and (5) that results in a second-order, nonlinear ordinary differential equation. Two boundary conditions are required to solve Eq. (11) and consist of the strand slip $s(x)$ and its derivative $s'(x)$ equal to zero at the end of the transfer length. The Runge-Kutta method was implemented to solve a second-order, nonlinear ordinary differential equation with a fine iterative step of 1/500 for the accuracy of the solution. The main steps of the solving procedure are briefly summarized in the flowchart shown in Figure 3.

$$u(x)C_S dx + A_c df_c = 0 \quad (7)$$

$$-u(x)C_S dx + A_s df_s = 0 \quad (8)$$

$$\frac{ds(x)}{dx} = \frac{df_s}{E_s} - \frac{df_c}{E_c} \quad (9)$$

$$\frac{d^2 s(x)}{dx^2} = \left(\frac{C_s}{E_s A_s} + \frac{C_s}{E_c A_c}\right) u(x) \quad (10)$$

$$s''(x) - \left(\frac{C_s}{E_s A_s} + \frac{C_s}{E_c A_c}\right) F_b \times s^{\alpha}(x) = 0 \quad (11)$$

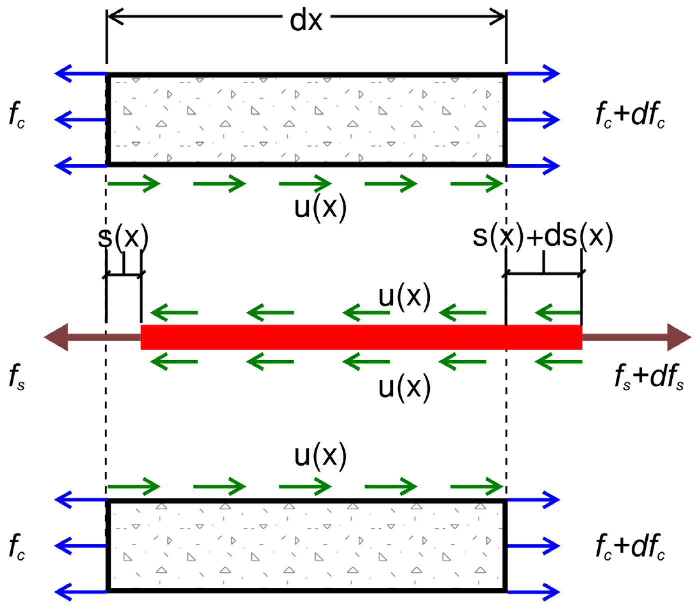


Figure 2 - Stresses distribution on element length *dx* (see *dx* position in Figure 1)

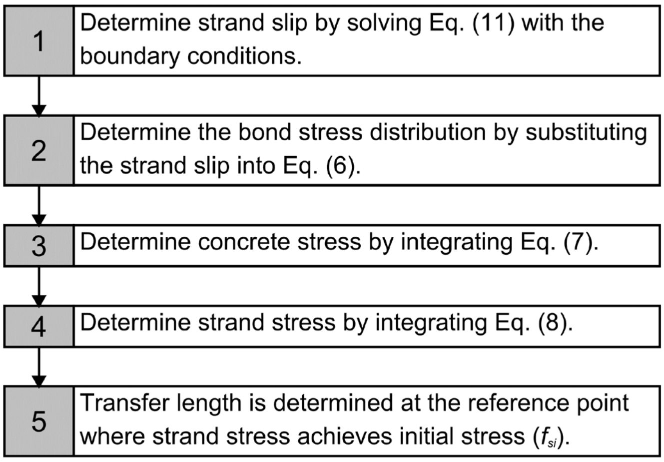


Figure 3 - Flowchart of transfer-length determination

To determine the short-term transfer length and bond-related parameters (i.e., strand end-slip and bond stress), the material properties at prestress transfer are used. These properties include concrete compressive strength, concrete modulus of elasticity and initial strand stress. At the long-term state, the long-term material properties are used, which include concrete compressive strength at 28 days of age, concrete modulus of elasticity at 28 days of age and effective strand stress after allowance for all prestress losses. Regarding the calibration coefficient $k_b$ introduced in Eq. (2), a value of 1.9 is used for the short-term predictions whereas a value of 1.0 is used for the long-term predictions as discussed in Section 6.3.

## 5. EXPERIMENTAL DATA

The experimental data are collected from two sources; one from a research project at the University of Arkansas, and the other one from the previous studies conducted at the University of Nebraska–Lincoln, the University of Tennessee–Knoxville, and the University of Texas–Austin.

### 5.1. University of Arkansas

The study involved casting twenty-four pretensioned concrete beams [47]. Four concrete mixtures were used to cast the beams as presented in Table 1. The mixtures were denoted by their type: N-CC for normal-strength conventional concrete, H-CC for high-strength conventional concrete, N-SCC for the normal-strength self-consolidating concrete, and H-SCC for high-strength self-consolidating concrete. The development of self-consolidating concrete complied with the thresholds required for precast prestressed concrete applications recommended by Khayat and Mitchell [48]. The compressive strength was tested using 100 mm by 200 mm cylinders. The average concrete compressive strength ranged from 41.0 MPa to 65.0 MPa at prestress transfer (1 day of age) and 63.0 MPa to 92.0 MPa at 28 days of age. The pretensioned concrete beams had a cross-section of 165 mm by 305 mm and a length of 5.4 m. All beams were cast with 18-mm, Grade 1860 prestressing strand. The prestressing strands were tensioned to $0.75f_{pu}$ prior to casting. Sixteen beams were cast with one strand, and eight beams were cast with two strands. The reinforcement details for the two beam configurations are shown in Figure 4-(1) and Figure 4-(2).

Two pretensioned concrete beams were cast simultaneously using one concrete batch. The beams were cured in the wooden forms for approximately one day. The sides of the forms were then unfolded which allowed the research team to take measurements, as shown in Figure 5-(1). A set of target points (steel discs) were glued onto the surface of the beams at the level of the prestressing strand on both sides and at both ends of the beams as typically illustrated on Figure 4-(3) and Figure 5-(2). Concrete strains were measured using 200-mm long demountable mechanical strain gauges (DEMEC) as shown in Figure 5-(3). The initial (zero strain) readings were recorded before prestress release. After gradually releasing the prestressing strand, the concrete strains were recorded immediately. The beams were then moved to a storage yard. The transfer length of the prestressing strand was determined from the measured concrete strain profile in combination with the 95% average maximum strain (AMS) method developed by Russell and Burns [49], which relies on the change in slope of the concrete strain profile. The distance from the member end (live or dead) to the point at which 95% average maximum strain is measured represents the corresponding transfer length of the prestressing strand.

A micrometer was used to measure strand slip at the end of prestressing strand through a metal clamp attached to the strand portion protruded from the beam ends, as typically illustrated in Figure 4-(3). The readings were taken at the same time concrete surface strains were measured. The nominal strand slip is the difference between the initial reading and the subsequent reading. The strand slip at prestress transfer was determined by subtracting the elastic shortening of the free strand portion from the nominal strand slip [50].

### 5.2. Other Universities

Tadros and Morcous [51] evaluated the transfer length of 18-mm prestressing strand in four prismatic specimens with different levels of reinforcing confinement. The prisms had a 178-mm square cross-section and were 2.4 m long. Self-consolidating concrete, which had a compressive strength of 41.4 MPa at release, was used to cast the prisms. One prestressing strand was placed at the center of each prism and tensioned to $0.75f_{pu}$. The measured transfer length at prestress transfer was 787 mm on average, which is 88% and 74% of the ACI 318 ($50d_b$ = 890 mm) and AASHTO ($60d_b$ = 1070 mm) limits, respectively. The effect of confinement was minimal on the measured transfer length.

Patzlaff *et al.* [52] measured the transfer length of 18-mm prestressing strand in eight 8.53-m long T-girders. The girder section was 610 mm deep, 200 mm wide at the stem, and 810 mm wide at the top flange. Each girder contained six prestressing strands tensioned to $0.75f_{pu}$. All girders were cast with self-consolidating concrete, which had a release-strength and 28-day strength of 63.5 MPa and 78.5 MPa, respectively. The average transfer length measured at prestress transfer was 527 mm. This transfer length is 59% and 49% in comparison to the ACI 318 ($50d_b$ = 890 mm) and AASHTO ($60d_b$ = 1070 mm) limits, respectively. On the other hand, similar to the observation on prism specimens [51], the confining reinforcement had no significant effect on the measured transfer length.

Maguire *et al.* [53] measured the transfer length for two full-scale double-Tee girders. The girder section was 502 mm deep, 2438 mm wide and 15.24 m long. High-strength self-consolidating concrete was used for the girder fabrication. The concrete had a compressive strength of 83 MPa release and 103 MPa at 28 days of age. Each stem of the girders contained ten 18-mm prestressing strands tensioned to $0.6f_{pu}$. The average measured transfer length at prestress transfer was 419 mm, which is significantly shorter than the ACI 318 ($50d_b$ = 890 mm) and AASHTO ($60d_b$ = 1070 mm) limits.

Table 1 - Concrete mixture proportions

| Concrete mixture | N-CC | H-CC | N-SCC | H-SCC |
|---|---|---|---|---|
| Cement, kg/m$^3$ | 415 | 415 | 460 | 489 |
| Coarse aggregate, kg/m$^3$ | 996 | 996 | 834 | 834 |
| Fine aggregate, kg/m$^3$ | 809 | 863 | 881 | 826 |
| Water, kg/m$^3$ | 166 | 145 | 184 | 196 |
| Water / Cement ratio *(w/cm)* | 0.4 | 0.35 | 0.4 | 0.4 |
| Slump flow, mm | N/A | N/A | 660 | 640 |
| Compressive strength at prestress transfer $f'_{ci}$ MPa | 43 | 63 | 41 | 54 |
| Compressive strength at 28 days of age $f'_c$, MPa | 66 | 92 | 63 | 73 |
| N-CC = normal-strength conventional concrete; H-CC = high-strength conventional concrete; N-SCC = normal-strength self-consolidating concrete; H-SCC =high-strength self-consolidating concrete. | | | | |

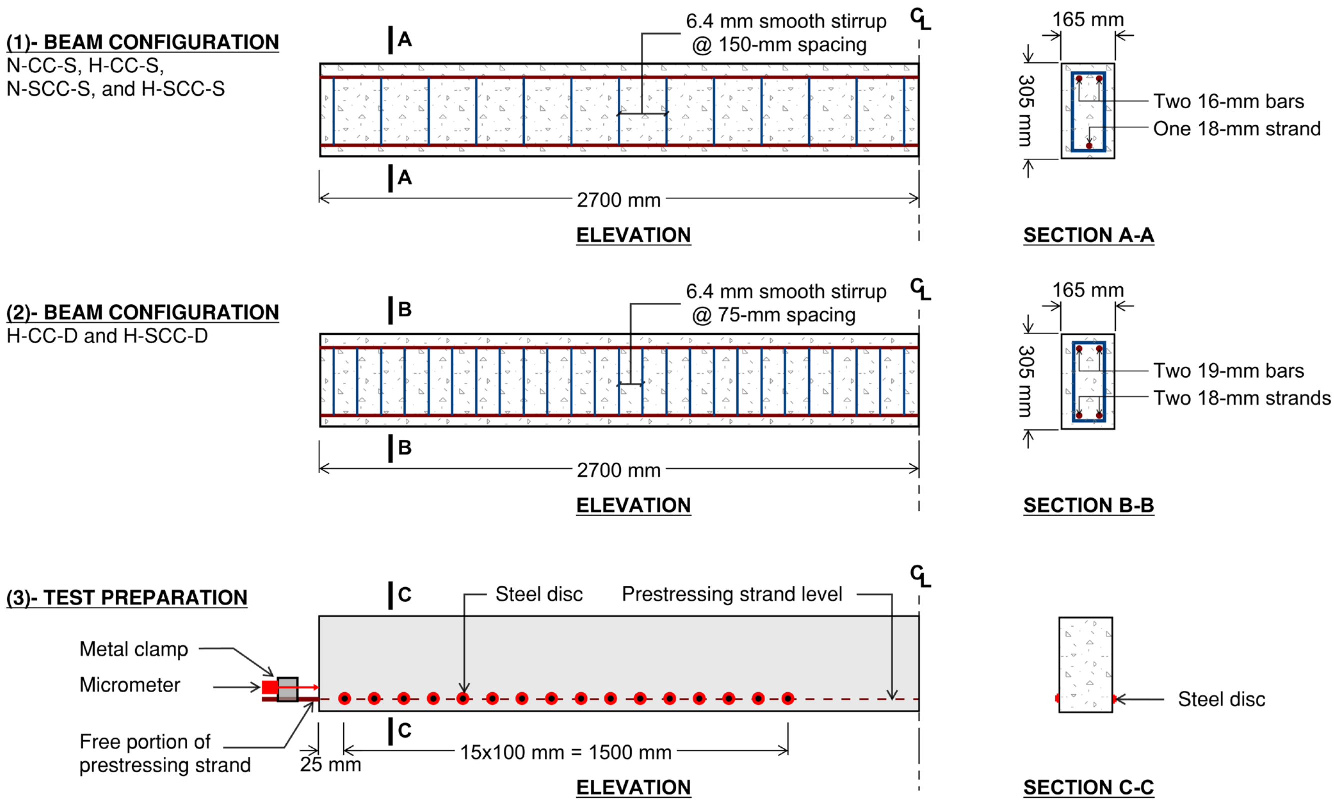


Figure 4 - Beam configurations and test setup for measurement of transfer length and strand slip

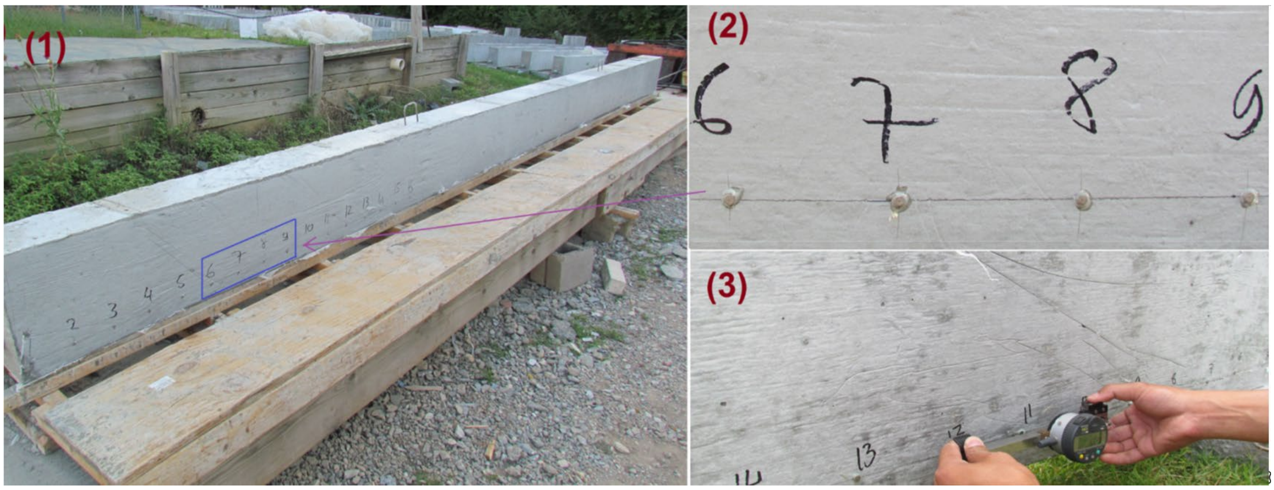


Figure 5 - Transfer length measurement: (1) attachment of target points on the surface of a pre-tensioned concrete beam after removing the form; (2) a set of target points placed at spacing of 100 mm; (3) use of mechanical strain gauge to record data

In related research, Song *et al.* [54] measured the transfer length and investigated the splitting force for two AASHTO Type I girders. Girder I was cast with 18-mm, Grade 1860 prestressing strand. Girder II was cast with 16-mm, Grade 2270 prestressing strand. High-strength self-consolidating concrete was used for fabrication of both girders. The concrete compressive strength at release was approximately 67 MPa. Each girder contained 12 prestressing strands tensioned to $0.75f_{pu}$. The measured transfer length of 18-mm prestressing strand at prestress transfer was 537 mm, which is 60% and 50% of the predicted values by ACI 318 ($50d_b$ = 890 mm) and AASHTO ($60d_b$ = 1070 mm) limits, respectively. In addition, the use of high-strength concrete was the key reason for the short transfer length in comparison to the code limits.

In another study, Morcous *et al.* [36] measured the transfer length of prestressing strand in two NU 1350 girders. The first girder was 34.0 m long and contained twenty-four 18-mm prestressing strand. The second girder was 43.0 m long and contained thirty-seven prestressing strands. For both girders, the prestressing strands were tensioned to $0.75f_{pu}$. The self-consolidating concrete reached 51.5 MPa and 71.4 MPa at one day and at 28 days of age, respectively. On average, the measure transfer length at prestress transfer was 810 mm, which is 91% and 76% of the predicted values for ACI 318 ($50d_b$ = 890 mm) and AASHTO ($60d_b$ = 1070 mm) limits, respectively.

Recently, Salazar *et al.* [55] investigated the structural behavior of the end-region for two Tx46 and two Tx70 girders. All girders were 9.0 m long. The Tx46-I and Tx46-II girders were 1168 mm deep and respectively contained twenty-four and thirty 18-mm prestressing strands. The concrete compressive strength at release was 39.3 MPa and 35.9 MPa for the first and second girder, respectively. The Tx70-I and Tx70-II were 1778 mm deep and contained twenty-eight and forty-two prestressing strands, respectively. The concrete compressive strength at release was 44.9 MPa and 57.3 MPa, respectively. All prestressing strands were tensioned to $0.75f_{pu}$. The measured transfer lengths at prestress transfer were 1062 mm, 814 mm, 914 mm, and 960 mm for the Tx46-I, Tx46-II, Tx70-I, and Tx70-II, respectively. In comparison to the code-predicted values, the measured transfer lengths were partially longer than the ACI 318 ($50d_b$ = 890 mm) and less than the AASHTO ($60d_b$ = 1070 mm) limits.

It should be noted that the end zones of the girders tested by Morcous *et al.* [36] and Salazar *et al.* [55] experienced cracking along the web and bottom flange during the prestress transfer stage.

As in this study, it is noteworthy that transfer lengths were determined by applying the 95% average maximum strain (AMS) method developed by Russell and Burns [49]. The experimental data were obtained from DEMEC strain gauges at 100 mm spacing [36,51,53,54] or at 50 mm spacing [52], and from electrical strain gauges installed on the strands at 150-300 mm [55] which required a modified version of the 95% AMS method.

## 6. ANALYSIS AND DISCUSSIONS

### 6.1. Transfer Length Verification

Figure 6 presents the measured transfer lengths at prestress transfer for the twenty-four pretensioned concrete beams tested at University of Arkansas. The predicted values of transfer length at prestress transfer (short-term) and after allowing for all prestress losses (long-term), which were accounted for by considering a final effective stress of $0.75f_{si}$, are also included, together with the limits from code provisions for transfer length. As it can be observed, the ACI 318 and AASHTO limits provide a conservative prediction for the transfer length (short- and long-term) from the perspective of the Ultimate Limit State design. On average, the measured transfer length is 71% and 59% of the ACI 318 and AASHTO limits, respectively. Eq. (1) provides a prediction similar to AASHTO. The overestimation of the code equations comes from two sources: (a) the code equations ignore the contribution of concrete strength; and (b) the prestressing strands exhibit good bond. It is worth noting that the analytical method considers both factors that improve the transfer-length prediction: on average, the measured transfer length at prestress transfer is 98% of the predicted values. The comparison to the previous studies from other universities revealed two different observations. The analytical method provides a good prediction for the measured transfer lengths at prestress transfer sourced from Tadros and Morcous [51], Patzlaff *et al.* [52], Maguire *et al.* [53], and Song *et al.* [54]. The measured transfer lengths are 103%, 92%, 87%, and 97% of the predicted values; assuming that the 3% exceeded in the first comparison is acceptable. On the other hand, the analytical method underestimates the measured transfer lengths of the pretensioned concrete girders investigated by Morcous *et al.* [36] and Salazar *et al.* [55]. The measured transfer lengths are 123% and 128% of the predicted values. This difference is most likely due to the cracking in the end zones which was previously mentioned.

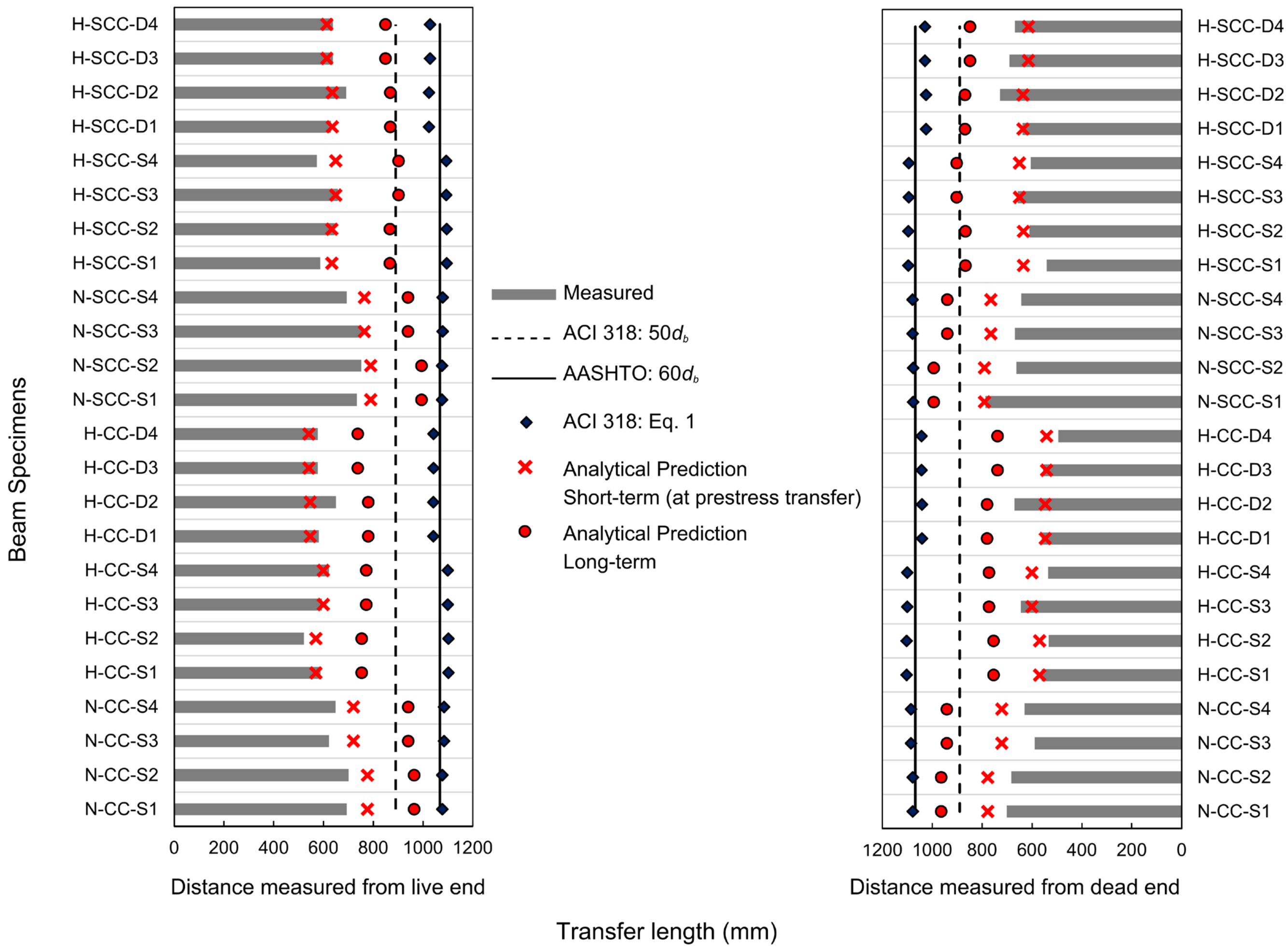


Figure 6 - Measured, analytical, and code-limit transfer lengths

## 6.2. Strand Slip Verification

Figure 7 presents the measured strand end slips at prestress transfer for the twenty-four pretensioned concrete beams tested at University of Arkansas. The predicted values of strand end slip at both short- and long-term stages are also included. In general terms, it can be observed that the measured and predicted short-term strand slip values ranged from 1.4 mm to 2.2 mm and 1.6 mm to 2.3 mm, respectively. The analytical bond model is able to capture this trend and provides a reasonable prediction for the experimental data. On average, the measured strand slip is 94% of the predicted values. This result ascertains that the strand slip is dependent on the concrete compressive strength.

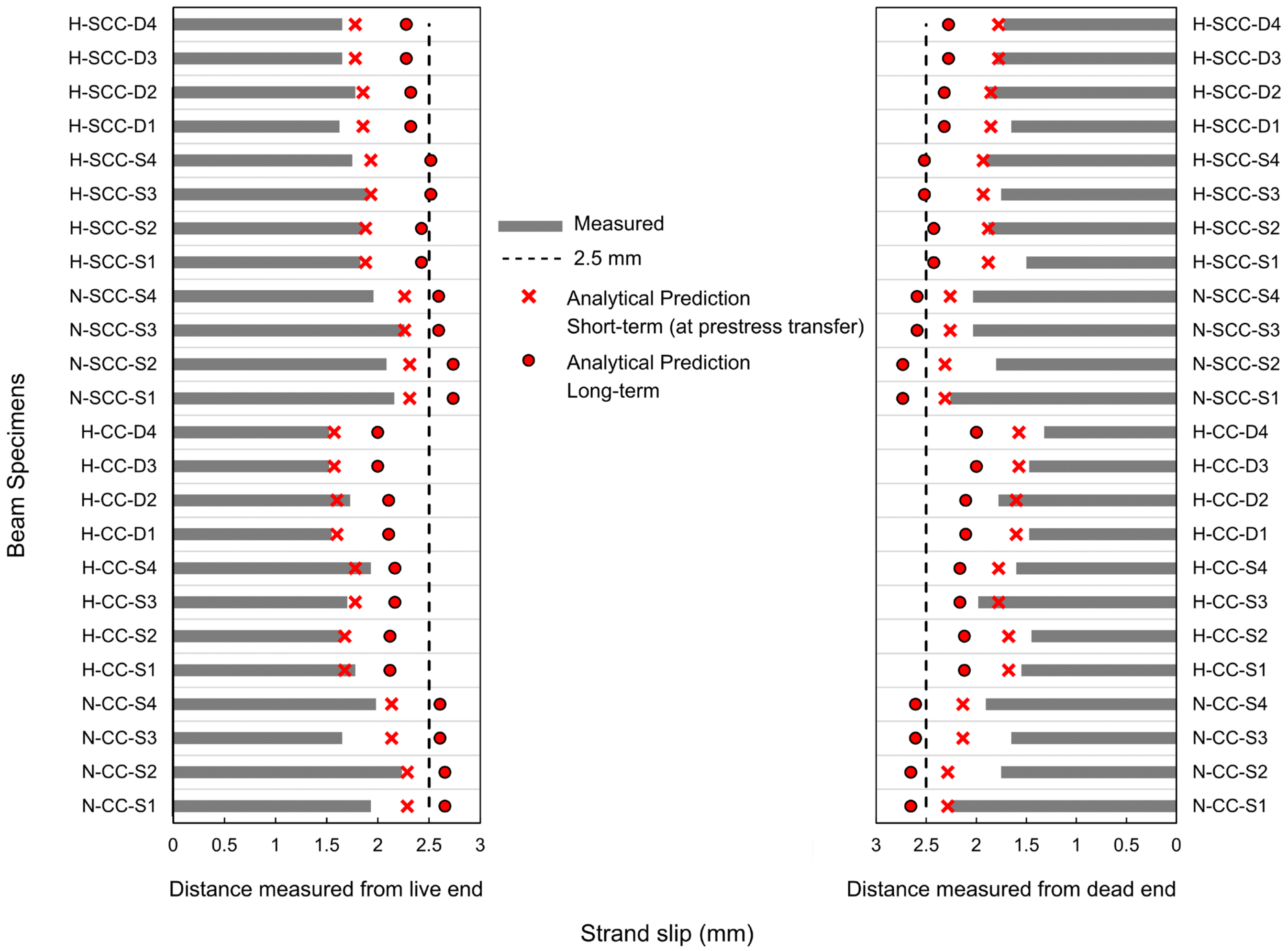


Figure 7 - Measured, analytical, and recommended threshold strand slip

The ACI 318 and AASHTO codes have no threshold for the strand slip even though several studies have demonstrated strand slip is a reliable indicator of strand bond [12,27,56]. Dang *et al.* [56] recommended a strand slip threshold of 2.5 mm based on the correlation of the strand end slip to the transfer and development length of prestressing strand. If a prestressing strand has slip at prestress transfer longer than 2.5 mm, the transfer length and development length is likely to be longer than the code limits; where development length is the required length for prestressing strands to develop $f_{ps}$; where $f_{ps}$ is the stress in the prestressing steel strand at the time for which the nominal flexural capacity of a member is required [33,57]. Therefore, the analytical determination of the strand end slip at the prestress transfer can provide an early indication of the transfer and development length of prestressing strands. This could then prevent a time-consuming and possibly costly experimental investigation.

### 6.3. Bond Stress Distribution

Figure 8 shows the bond stress distribution of beam specimen N-CC-S1. Part 1 at the upper portion of the graph presents the bond stress distribution in a nonlinear form. The bond stress is at a maximum at the beginning and reduces toward the end of the transfer zone. At this point the prestressing strand fully transfers the prestress force to concrete. Part 2 at the lower portion of the graph presents the equivalent bond stress, which is uniform in the transfer zone. The bond magnitude is determined by integrating the bond stress distribution in Part 1 and then dividing by the associated transfer length.

Part 1 of Figure 8 presents the short- and long-term bond stress distribution. At this stage, Hoyer's effect and mechanical interlock (i.e., calibration coefficient $k_b$ of 1.9 as aforementioned) contribute to strand bond. The predicted transfer length is 777 mm. For the long-term determination, under the effect of concrete creep and shrinkage in the transverse direction, the concrete adjacent to the prestressing strand deforms as it is subjected to the compressive stresses generated by the lateral expansion of prestressing strand [44]. Therefore, the contribution of Hoyer's effect is assumed minimal whereas the mechanical interlock becomes the main contributor to strand bond (i.e., calibration coefficient $k_b$ reduces to 1.0). Simultaneously, the pretensioned concrete member experiences longitudinal deformation due to concrete creep and shrinkage which results in prestress losses. Additional degradation or deterioration of the pretensioned concrete members which may occur can also affect the bond between the prestressing strand and concrete (e.g. strand corrosion). As a result, the magnitude of the maximum bond stress at the beginning of the transfer zone decreases with time, but the transfer zone increases. The predicted transfer length at this stage (long-term, without degradation/deterioration) of the beam specimen N-CC-S1 is 964 mm, which is 24% longer than the predicted value at the prestress transfer stage. For all beam specimens, the increase in transfer length ranged from 23% to 43% with an average of 33% as presented in Figure 6. This range is greater than the increase observed in the 13-mm and 15-mm prestressing strands, which typically ranges from 10%-20% [11,58]. The result shown in Figure 6 also indicates the ACI 318 limit of $50d_b$ is not conservative in predicting the long-term transfer length. This finding reveals that the limit of $50d_b$ is conservative for predicting the transfer length at prestress transfer, but not necessarily for the long-term transfer length. On the other hand, the ACI 318's Eq. (1) and AASHTO limit of $60d_b$ provide a conservative prediction.

As shown in Part 2 of Figure 8, the equivalent bond stress at the short- and long-term is 5.56 MPa and 4.21 MPa. The ACI 318 bond stress (2.76 MPa or 400 psi) is less than the equivalent bond stresses. This is the source for the conservative prediction of Eq. (1) for the short-term transfer length as shown in Figure 6. In terms of applications, determination of the equivalent bond stress is beneficial in finite-element modeling of pretensioned concrete members. If the location of interest is beyond the transfer zone, the equivalent bond stress can be used to reduce the computational effort. This is the case when calculating the ultimate flexural load capacity of pretensioned concrete members, when the location of interest is typically at the mid-span of the members [59–61]. Otherwise, if the location of interest is within the transfer zone, it is needed to accurately simulate bond stress distribution.

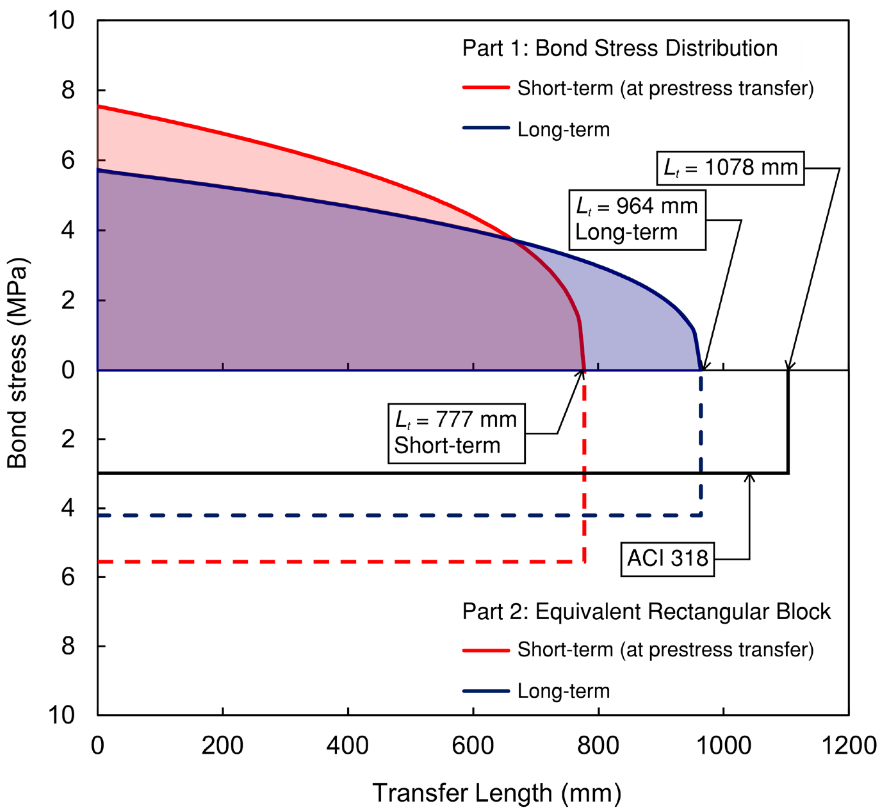


Figure 8 - Bond stress distribution along the transfer length of beam specimen N-CC-S1

## 6.4. Strand Slip Distribution

Research commonly focuses on measuring strand end slip immediately after prestress transfer. It is known that strand slip is a maximum at the free end and decreases as one moves closer toward the end of the transfer zone. It is noteworthy that by having a better understanding of the strand slip distribution in that region, one has a better understanding of the behavior of prestressing strand in the transfer zone. Figure 9 presents the slip distribution of beam specimen N-CC-S1. The slip distribution of the strand is nonlinear in the transfer zone. For verification purpose, the slip distribution along the short-term transfer length was compared to the one proposed by Martí-Vargas *et al.* [42] as expressed in Eq. (12), which was obtained from an experimental basis, where $s(x)$ is the strand slip at location $x$ from the free end of the pretensioned member.

$$s(x) = 8.7\frac{\left(L_t - x\right)^2}{L_t^2\sqrt{f_{ci}^{'}}} \tag{12}$$

As observed in Figure 9, both distribution curves are generally in agreement, regardless of a slight difference at the beginning of the transfer zone. The analytical method developed in this study provides a closer prediction to the experimental data. In comparison to the experimental results, the variation in the strand slip predictions is +0.11 mm in this study and -0.28 mm for Martí-Vargas *et al.* [42]. In fact, it is worth mentioning that Martí-Vargas *et al.* [42] studied the slip distribution of 13-mm prestressing strand. Therefore, based on ACI 318 [33] and AASHTO [35] provisions —transfer length is linearly proportional to strand diameter— and the Guyon's theory [42] —transfer length is linearly proportional to strand end slip—, a ratio of strand diameters (18-mm/13-mm=1.4) was applied for consistent comparison.

The results shown in Figure 9 indicated that strand slip increases over time. In comparison to the short-term strand slip, the long-term strand slip of beam specimen N-CC-S1 increases 0.47 mm, which is 20.5% of the short-term slip. Similar to the increase observed in the transfer length, concrete creep and shrinkage are the two dominant contributors. For all beam specimens, the increase ranged from 15% to 32% with an average of 24% as presented in Figure 7. This finding confirms the assumption of the minimal contribution of the adhesion to strand bond as aforementioned. The prestressing strand in the transfer zone tends to slip gradually over time, therefore any adhesion bond formed between the two materials would be broken or fractured.

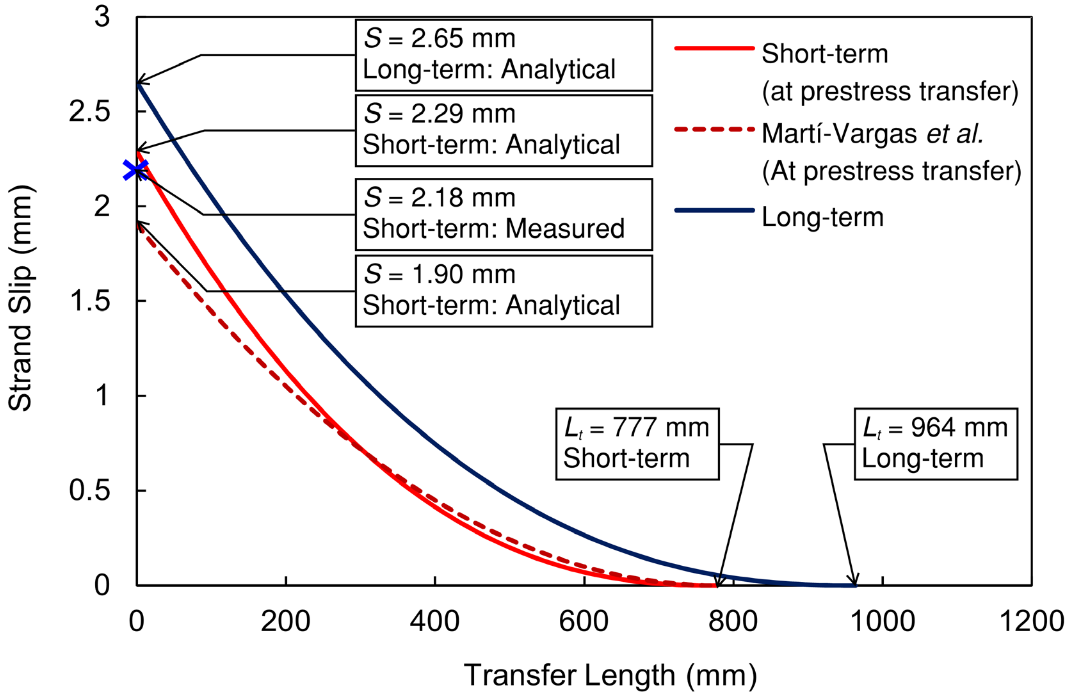


Figure 9 - Strand slip distribution along the transfer length of beam specimen N-CC-1

## 6.5. Strand Stress Variation

The variation of strand stress is presented in Figure 10. Due to the nonlinear distribution of the strand bond (refer to Figure 8), the strand stress varies nonlinearly in the transfer zone. However, ACI 318 assumes a linear strand stress as shown in Figure 1. This assumption has two implications. First, at a given location within the transfer zone, the strand stress is greater than the assumed value as denoted by the "Strand Stress Difference" in Figure 10. In other words, the prestress force transferred to the concrete is greater than the code-predicted value. This could potentially lead to concrete cracking in the transfer zone. Second, the interaction between multiple prestressing strands in the transverse direction is more severe. As graphically visualized by Dang *et al.* [62], each prestressing strand has a 'cylindrical transfer zone' to transfer the prestress force to the adjacent concrete. When several 18-mm prestressing strands are placed in a grid pattern, the cylindrical transfer zones of these strands are partially overlapped near the beginning of the transfer zone. The tensile stress is greater in the overlapped regions and results in concrete cracking if the tensile stress is greater than the concrete tensile strength. In fact, a linear strand stress variation was assumed by Dang *et al.* to investigate the intensified tensile stress in the overlapped region. When considering the nonlinear strand stress variation observed in this study, the extension of the overlapped region is greater than expected, which increases the concrete region prone to cracking. This is likely to be another factor for the long transfer length observed in Morcous *et al.* [36] and Salazar *et al.* [55] studies, where the prestressing strands were placed at a grid pattern of 51x51 mm.

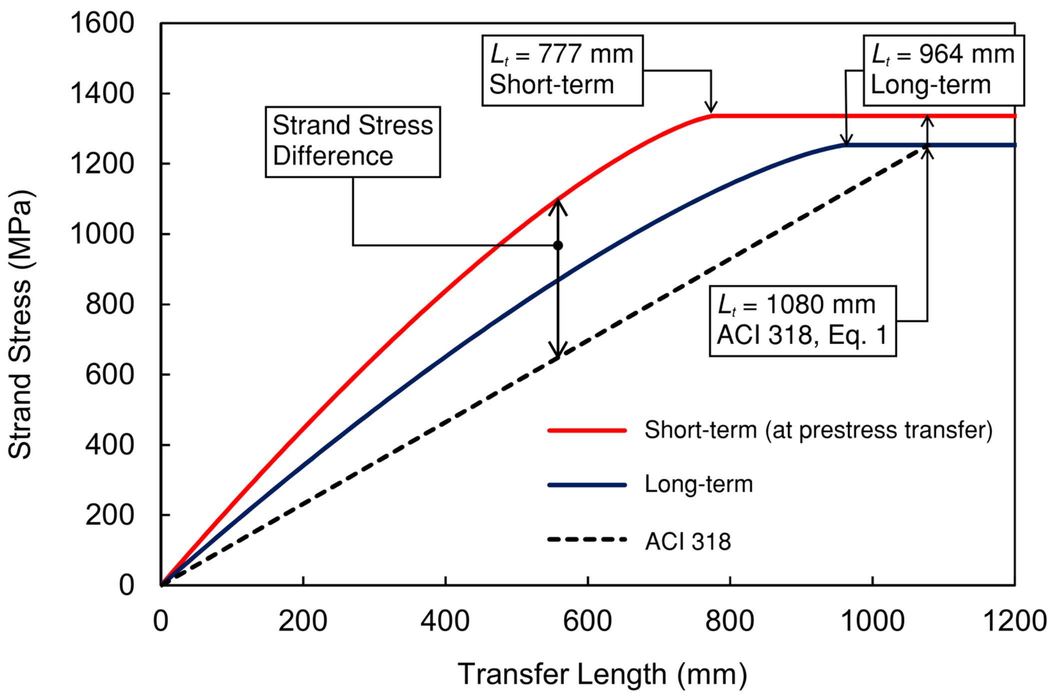


Figure 10 - Strand stress variation along the transfer length of beam specimen N-CC-1

## 6.6. Research Limitations

The developed bond model excluded the effect of transverse reinforcement to the transfer length of prestressing strands. Generally it is understood that transverse reinforcement can provide a confining effect to the concrete in compression. Warenycia *et al.* [63] analytically quantified the contribution of transverse reinforcement in confining the concrete in the transfer zone which shortens the transfer length of prestressing strand. In fact, Maguire [51] and Patzlaff *et al.* [52] experimentally found minimal to no contribution of transverse reinforcement as mentioned in the previous discussions. Additional research is needed, particularly in testing large-scale pretensioned concrete girders, to fully understanding the effect of transverse reinforcement. Additionally, more experimental data (i.e., long-term transfer length and strand end-slip) are required and could be valuable to validate the proposed model in this study.

## 7. CONCLUSIONS

The following conclusions can be made based on the investigation on the strand bond of 18-mm prestressing strand:

- An analytical bond model has been developed for 18-mm prestressing strand. Through utilization of STSB results, the model considers the effect of concrete compressive strength on the bond performance. A coefficient of 1.9 is suitable for calibrating the difference in the bond mechanism of pretensioned and non-pretensioned 18-mm prestressing strands.
- The assumption regarding a minimal contribution of the adhesion to the strand bond in the transfer zone has been confirmed. The prestressing strand tends to slip gradually over time, so any kind of bond by adhesion formed between prestressing strand and concrete would be fractured.
- The developed analytical model provides a good prediction for the transfer length measured in pretensioned concrete beams. The measured transfer length is 98% of the

value predicted by the analytical model. For medium-scale pretensioned concrete girders, the analytical model can provide a reasonable prediction. However, the model underestimates the transfer length of large-scale pretensioned concrete girders due to cracking in the transfer zone.

- Transfer length increases over time. The long-term transfer length is 33% longer than the short-term. The ACI 318 Eq. (1) and AASHTO limit ($60d_b$) adequately predict the short- and long-term transfer lengths. The ACI 318 limit of $50d_b$ is conservative for predicting the short-term transfer length but not necessarily conservative for the long-term transfer length.
- The bond stress distribution is nonlinear in the transfer zone. In comparison to the short-term bond stress distribution, the maximum long-term bond stress is decreased, but the extension of the transfer zone is increased.
- The short-term strand slip is reasonably predicted by the analytical model. The measured strand slip is 94% of the predicted values. In comparison to the short-term strand slip, the long-term strand slip is 24% greater on average.
- The strand slip distribution is nonlinear in the transfer zone. The slip is maximum at the beginning of the transfer zone (free end of the member) and reduces toward the end of the transfer zone. The variation of the short- and long-term strand slip is similar.
- The strand stress variation in the transfer zone is nonlinear, which is not in agreement with the ACI design code assumption. At a given location within the transfer zone, the prestress transfer to the concrete is greater than the code-predicted value. This observation posts a concern regarding concrete cracking in the transfer zone of pretensioned concrete members.

## ACKNOWLEDGEMENTS

This research is supported by the University of Arkansas at Fayetteville. The authors gratefully acknowledge to several graduate researchers at the University of Arkansas in assisting with the experimental work.

## NOTATIONS

$\alpha$ = exponential coefficient of bond stress-slip model

$A_c$ = area of concrete, mm$^2$

$A_s$ = cross-sectional area of prestressing strand, mm$^2$

$C_s$ = strand perimeter, mm

$E_c$ = concrete modulus of elasticity, MPa

$E_s$ = steel modulus of elasticity, MPa

$d_b$ = nominal strand diameter, mm

$F_b$ = bond magnitude

$f_c$ = concrete stress, MPa

$f'_{ci}$ = concrete compressive strength at 1 day of age, MPa

$f'_c$ = concrete compressive strength at 28 days of age, MPa

$f_s$ = strand stress, MPa

$f_{si}$ = initial stress, MPa

$f_{se}$ = effective stress, MPa

$f_{pu}$ = ultimate stress, MPa

$k_b$ = calibration coefficient

$L_t$ = transfer length, mm

$P_f$ = pullout force corresponding to free end slip of 2.5 mm (0.1 in.), kN

$P_i$ = pullout force corresponding to free end slip of 0.25 mm (0.01 in.), kN

$s(x)$ = strand slip at location $x$

$s_f$ = strand slip at free end of 2.5 mm (0.1 in.)

$s_i$ = strand slip at free end of 0.25 mm (0.01 in.)

$u(x)$ = bond stress at location $x$

$u_f$ = average bond stress corresponding to pullout force of $P_f$, MPa

$u_i$ = average bond stress corresponding to pullout force of $P_i$, MPa

## REFERENCES


[1] G. Morcous, A. Hatami, M. Maguire, K. Hanna, M.K. Tadros, Mechanical and Bond Properties of 18-mm- (0.7-in.-) Diameter Prestressing Strands, J. Mater. Civ. Eng. 24 (2012) 735–744. https://doi.org/10.1061/(ASCE)MT.1943-5533.0000424.

[2] J.K. Kim, T.R. Seong, K.P. Jang, S.H. Kwon, Tensile behavior of new 2,200 MPa and 2,400 MPa strands according to various types of mono anchorage, Struct. Eng. Mech. 47 (2013) 383–399. https://doi.org/10.12989/SEM.2013.47.3.383.

[3] J.M. Yang, H.J. Yim, J.K. Kim, Transfer length of 2400 MPa seven-wire 15.2 mm steel strands in high-strength pretensioned prestressed concrete beam, Smart Struct. Syst. 17 (2016) 577–591. https://doi.org/10.12989/SSS.2016.17.4.577.

[4] J.S. Lawler, J.D. Connolly, A.E.N. Osborn, Acceptance Tests for Surface Characteristics of Steel Strands in Prestressed Concrete, National Academies Press, 2009. https://doi.org/10.17226/14206.

[5] C.N. Dang, C.D. Murray, R.W. Floyd, W.M. Hale, J.R. Mart?-Vargas, Correlation of strand surface quality to transfer length, ACI Struct. J. 111 (2014).

https://doi.org/10.14359/51686925.

[6] V. Briere, K.A. Harries, J. Kasan, C. Hager, Dilation behavior of seven-wire prestressing strand – The Hoyer effect, Constr. Build. Mater. 40 (2013) 650–658. https://doi.org/10.1016/J.CONBUILDMAT.2012.11.064.

[7] B.W. Russell, N.H. Burns, DESIGN GUIDELINES FOR TRANSFER, DEVELOPMENT AND DEBONDING OF LARGE DIAMETER SEVEN WIRE STRANDS IN PRETENSIONED CONCRETE GIRDERS. FINAL REPORT, Austin, 1993. https://trid.trb.org/view/379831 (accessed February 19, 2022).

[8] C.D. Buckner, Review of strand development length for pretensioned concrete members, PCI J. 40 (1995) 84–105. https://doi.org/10.15554/PCIJ.03011995.84.105.

[9] J. Ramirez, B. Russell, Transfer, Development, and Splice Length for Strand/Reinforcement in High-Strength Concrete, Transportation Research Board, 2008. https://doi.org/10.17226/13916.

[10] D. Mitchell, W.D. Cook, T. Tham, Influence of High Strength Concrete on Transfer and Development Length of Pretensioning Strand, PCI J. 38 (1993) 52–66. https://doi.org/10.15554/PCIJ.05011993.52.66.

[11] R.W. Barnes, J.W. Grove, N.H. Burns, Experimental Assessment of Factors Affecting Transfer Length, Struct. J. 100 (2003) 740–748. https://doi.org/10.14359/12840.

[12] B.H. Oh, S.N. Lim, M.K. Lee, S.W. Yoo, Analysis and Prediction of Transfer Length in Pretensioned, Prestressed Concrete Members, Struct. J. 111 (2014) 549–560. https://doi.org/10.14359/51686571.

[13] A.T. Ramirez-Garcia, R.W. Floyd, W. Micah Hale, J.R. Martí-Vargas, Influence of concrete strength on development length of prestressed concrete members, J. Build. Eng. 6 (2016) 173–183. https://dx.doi.org/10.1016/j.jobe.2016.03.005.

[14] M. Arezoumandi, K.B. Looney, J.S. Volz, An experimental study on transfer length of prestressing strand in self-consolidating concrete, Eng. Struct. 208 (2020) 110317. https://doi.org/10.1016/J.ENGSTRUCT.2020.110317.

[15] M. Arezoumandi, K.B. Looney, J.S. Volz, Bond performance of prestressing strand in self-consolidating concrete, Constr. Build. Mater. 232 (2020) 117125. https://doi.org/10.1016/J.CONBUILDMAT.2019.117125.

[16] M. Arezoumandi, K.B. Looney, J.S. Volz, Development length of prestressing strand in self-consolidating concrete vs. conventional concrete: Experimental study, J. Build. Eng. 29 (2020) 101218. https://doi.org/10.1016/J.JOBE.2020.101218.

[17] A.A. Arab, S.S. Badie, M.T. Manzari, A methodological approach for finite element modeling of pretensioned concrete members at the release of pretensioning, Eng. Struct. 33 (2011) 1918–1929. https://doi.org/10.1016/J.ENGSTRUCT.2011.02.028.

[18] P. Okumus, M.G. Oliva, S. Becker, Nonlinear finite element modeling of cracking at ends of pretensioned bridge girders, Eng. Struct. 40 (2012) 267–275. https://doi.org/10.1016/J.ENGSTRUCT.2012.02.033.

[19] A.O. Abdelatif, J.S. Owen, M.F.M. Hussein, Modelling the prestress transfer in pre-tensioned concrete elements, Finite Elem. Anal. Des. 94 (2015) 47–63. https://doi.org/10.1016/J.FINEL.2014.09.007.

[20] O. Yapar, P.K. Basu, N. Nordendale, Accurate finite element modeling of pretensioned prestressed concrete beams, Eng. Struct. 101 (2015) 163–178. https://doi.org/10.1016/J.ENGSTRUCT.2015.07.018.

[21] R. Steensels, L. Vandewalle, B. Vandoren, H. Degée, A two-stage modelling approach for the analysis of the stress distribution in anchorage zones of pre-tensioned, concrete elements, Eng. Struct. 143 (2017) 384–397.

https://doi.org/10.1016/J.ENGSTRUCT.2017.04.011.

[22] K. Van Meirvenne, W. De Corte, V. Boel, L. Taerwe, Non-linear 3D finite element analysis of the anchorage zones of pretensioned concrete girders and experimental verification, Eng. Struct. 172 (2018) 764–779. https://doi.org/10.1016/J.ENGSTRUCT.2018.06.065.

[23] B.H. Oh, E.S. Kim, Y.C. Choi, Theoretical Analysis of Transfer Lengths in Pretensioned Prestressed Concrete Members, J. Eng. Mech. 132 (2006) 1057–1066. https://doi.org/10.1061/(ASCE)0733-9399(2006)132:10(1057).

[24] J.M. Benítez, J.C. Gálvez, Bond modelling of prestressed concrete during the prestressing force release, Mater. Struct. 1 (2011) 263–278. https://doi.org/10.1617/S11527-010-9625-5.

[25] M. Markovič, N. Krauberger, M. Saje, I. Planinc, S. Bratina, Non-linear analysis of pre-tensioned concrete planar beams, Eng. Struct. 46 (2013) 279–293. https://doi.org/10.1016/J.ENGSTRUCT.2012.08.004.

[26] S.J. Han, D.H. Lee, S.H. Cho, S.B. Ka, K.S. Kim, Estimation of transfer lengths in precast pretensioned concrete members based on a modified thick-walled cylinder model, Struct. Concr. 17 (2016) 52–62. https://doi.org/10.1002/SUCO.201500049.

[27] F. Bai, J.S. Davidson, Composite beam theory for pretensioned concrete structures with solutions to transfer length and immediate prestress losses, Eng. Struct. 126 (2016) 739–758. https://doi.org/10.1016/J.ENGSTRUCT.2016.08.031.

[28] C. Lee, S. Lee, S. Shin, Modeling of Transfer Region with Local Bond-Slip Relationships, Struct. J. 114 (2017) 187–196. https://doi.org/10.14359/51689253.

[29] N. Fabris, F. Faleschini, C. Pellegrino, Bond Modelling for the Assessment of Transmission Length in Prestressed-Concrete Members, CivilEng 2020, Vol. 1, Pages

75-92. 1 (2020) 75–92. https://doi.org/10.3390/CIVILENG1020006.

[30] H. Park, Z.U. Din, J.Y. Cho, Methodological Aspects in Measurement of Strand Transfer Length in Pretensioned Concrete, Struct. J. 109 (2012) 625–634. https://doi.org/10.14359/51684040.

[31] W. Zhao, B.T. Beck, R.J. Peterman, C.H.J. Wu, Development of a 5-Camera Transfer Length Measurement System for Real-Time Monitoring of Railroad Crosstie Production, 2013 Jt. Rail Conf. JRC 2013. (2013). https://doi.org/10.1115/JRC2013-2468.

[32] S.J. Jeon, H. Shin, S.H. Kim, S.Y. Park, J.M. Yang, Transfer Lengths in Pretensioned Concrete Measured Using Various Sensing Technologies, Int. J. Concr. Struct. Mater. 13 (2019) 1–16. https://doi.org/10.1186/S40069-019-0355-Y/FIGURES/15.

[33] ACI CODE-318-19: Building Code Requirements for Structural Concrete and Commentary, (n.d.). https://www.concrete.org/store/productdetail.aspx?ItemID=318U19&Language=English (accessed February 19, 2022).

[34] C.N. Dang, J.R. Martí-Vargas, W.M. Hale, C.N. Dang, J.R. Martí-Vargas, W.M. Hale, Structural Engineering and Mechanics, Struct. Eng. Mech. 76 (2020) 67. https://doi.org/10.12989/SEM.2020.76.1.067.

[35] American Association of State Highway and Transportation Officials, AASHTO LRFD Bridge Design Specifications, 9th Edition, 2020. https://trid.trb.org/view/1704698 (accessed February 19, 2022).

[36] G. Morcous, S. Assad, A. Hatami, M.K. Tadros, Implementation of 0.7 in. diameter strands at 2.0 × 2.0 in. spacing in pretensioned Bridge girders, PCI J. 59 (2014) 145–158. https://doi.org/10.15554/PCIJ.06012014.145.158.

[37] G. Schuler, Producer's Experience with 10,000 psi Concrete and 0.7-in. Diameter Strands - Concrete Bridge Views, Concr. Bridg. Views. 54 (2009) 9–11. http://concretebridgeviews.com/2009/03/producers-experience-with-10000-psi-concrete-and-0-7-in-diameter-strands/ (accessed February 19, 2022).

[38] ASTM A1081/A1081M-21, Standard Test Method for Evaluating Bond of Seven-Wire Steel Prestressing Strand, West Conshohocken, 2021. https://www.astm.org/a1081_a1081m-21.html (accessed February 19, 2022).

[39] G.L. Balazs, Transfer Control of Prestressing Strands, PCI J. 37 (1992) 60–71. https://doi.org/10.15554/PCIJ.11011992.60.71.

[40] J.A. den Uijl, Bond Modelling of Prestressing Strand, Spec. Publ. 180 (1998) 145–170. https://doi.org/10.14359/5876.

[41] H. Park, J.Y. Cho, Bond-Slip-Strain Relationship in Transfer Zone of Pretensioned Concrete Elements, Struct. J. 111 (2014) 503–514. https://doi.org/10.14359/51686567.

[42] J.R. Martí-Vargas, W.M. Hale, E. García-Taengua, P. Serna, Slip distribution model along the anchorage length of prestressing strands, Eng. Struct. 59 (2014) 674–685. https://doi.org/10.1016/J.ENGSTRUCT.2013.11.032.

[43] C.N. Dang, R.W. Floyd, C.D. Murray, W.M. Hale, J.R. Mart?-Vargas, Bond stress-slip model for 0.6 in. (15.2 mm) diameter strand, ACI Struct. J. 112 (2015). https://doi.org/10.14359/51687750.

[44] R.S. Kareem, A. Al-Mohammedi, C.N. Dang, C.N. Dang, J.R. Martí-Vargas, W.M. Hale, Bond model of 15·2 mm strand with consideration of concrete creep and shrinkage, Https://Doi.Org/10.1680/Jmacr.18.00506. 72 (2020) 799–810. https://doi.org/10.1680/JMACR.18.00506.

[45] A. Pozolo, B. Andrawes, Analytical prediction of transfer length in prestressed self-

consolidating concrete girders using pull-out test results, Constr. Build. Mater. 25 (2011) 1026–1036. https://doi.org/10.1016/J.CONBUILDMAT.2010.06.076.

[46] M. Tadros, G. Morcous, Impact of Large 0.7 Inch Strand on NU-I Girders, Lincoln, NE, 2011. https://digitalcommons.unl.edu/matcreports/48 (accessed February 19, 2022).

[47] C. Dang, Measurement of Transfer and Development Lengths of 0.7 in. Strands on Pretensioned Concrete Elements, University of Arkansas, 2015. https://scholarworks.uark.edu/etd/1076 (accessed February 19, 2022).

[48] K.H. Khayat, D. Mitchell, Self-Consolidating Concrete for Precast, Prestressed Concrete Bridge Elements, National Academies Press, Washington, DC, 2009. https://doi.org/10.17226/14188.

[49] B.W. Russell, N.H. Bums, Measured transfer lengths of 0.5 and 0.6 in. Strands in pretensioned concrete, PCI J. 41 (1996) 44–64. https://doi.org/10.15554/PCIJ.09011996.44.65.

[50] C.N. Dang, W.M. Hale, J.R. Martí-Vargas, Assessment of transmission length of prestressing strands according to fib Model Code 2010, Eng. Struct. 147 (2017). https://doi.org/10.1016/j.engstruct.2017.06.019.

[51] M. Tadros, G. Morcous, Impact of 0.7 inch Diameter Strands on NU I-Grinders, Lincoln, NE, 2011. https://digitalcommons.unl.edu/ndor/88 (accessed February 19, 2022).

[52] Q. Patzlaff, G. Morcous, K. Hanna, M.K. Tadros, Bottom Flange Confinement Reinforcement in Precast Prestressed Concrete Bridge Girders, J. Bridg. Eng. 17 (2012) 607–616. https://doi.org/10.1061/(ASCE)BE.1943-5592.0000287.

[53] M. Maguire, G. Morcous, M.K. Tadros, Structural Performance of Precast/Prestressed

Bridge Double-Tee Girders Made of High-Strength Concrete, Welded Wire Reinforcement, and 18-mm-Diameter Strands, J. Bridg. Eng. 18 (2013) 1053–1061. https://doi.org/10.1061/(ASCE)BE.1943-5592.0000458.

[54] W. Song, Z.J. Ma, J. Vadivelu, E.G. Burdette, Transfer Length and Splitting Force Calculation for Pretensioned Concrete Girders with High-Capacity Strands, J. Bridg. Eng. 19 (2014) 04014026. https://doi.org/10.1061/(ASCE)BE.1943-5592.0000566.

[55] J. Salazar, H. Yousefpour, R.A. Abyaneh, H. Kim, A. Katz, T. Hrynyk, O. Bayrak, End-Region Behavior of Pretensioned I-Girders Employing 0.7 in. (17.8 mm) Strands, Struct. J. 115 (2018) 91–102. https://doi.org/10.14359/51700783.

[56] C.N. Dang, W.M. Hale, R.W. Floyd, J.R. Martí-Vargas, Prediction of development length from free-end slip in pretensioned concrete members, Mag. Concr. Res. 70 (2018). https://doi.org/10.1680/jmacr.17.00334.

[57] Precast-Prestressed Concrete Institute, PCI Design Handbook, 2017. https://www.pci.org/ItemDetail?iProductCode=MNL-120-17#1 (accessed February 20, 2022).

[58] L.A. Caro, J.R. Martí-Vargas, P. Serna, Time-dependent evolution of strand transfer length in pretensioned prestressed concrete members, Mech. Time-Dependent Mater. 4 (2013) 501–527. https://doi.org/10.1007/S11043-012-9200-2.

[59] L. Chen, B.A. Graybeal, Modeling Structural Performance of Second-Generation Ultrahigh-Performance Concrete Pi-Girders, J. Bridg. Eng. 17 (2012) 634–643. https://doi.org/10.1061/(ASCE)BE.1943-5592.0000301.

[60] G. Zhang, B.A. Graybeal, Development of UHPC Pi-Girder Sections for Span Length up to 41 m, J. Bridg. Eng. 20 (2015) 04014068. https://doi.org/10.1061/(ASCE)BE.1943-5592.0000653.

[61] C.D. Murray, M. Diaz Arancibia, P. Okumus, R.W. Floyd, Destructive testing and computer modeling of a scale prestressed concrete I-girder bridge, Eng. Struct. 183 (2019) 195–205. https://doi.org/10.1016/J.ENGSTRUCT.2019.01.018.

[62] C.N. Dang, R.W. Floyd, W.M. Hale, J.R. Martí-Vargas, Spacing requirements of 0.7 in. (18 mm) diameter prestressing strands, PCI J. 61 (2016). https://doi.org/10.15554/pcij.01012016.70-87.

[63] K. Warenycia, M. Diaz-Arancibia, P. Okumus, Effects of confinement and concrete nonlinearity on transfer length of prestress in concrete, Structures. 11 (2017) 11–21. https://doi.org/10.1016/J.ISTRUC.2017.04.002.